Chapter

Integrated Optical Coherence Tomography and Deep Learning for Evaluating of the Injectable Hydrogel on Skin Wound Healing

Qingliang Zhao and Lin Chen

Abstract

Recently hydrogels and the treatment of skin wounds based on hydrogel dressings have become one of the research hotspots in the field of skin trauma. In this chapter, we focus on the materials and methods of hydrogel preparation, and discuss the properties that hydrogels should possess for the treatment of wounds. Moreover, we discuss the potential of non-invasive optical imaging techniques in the assessment of cutaneous wound healing. The research results of the application of non-invasive optical techniques such as diffuse reflectance spectroscopy (DRS) and optical coherence tomography (OCT) in scar identification, skin bruising, and skin and vascular structure identification are reviewed. Furthermore, we further discuss the superiority and potential of current artificial intelligence (AI) technology in dermatological diagnosis, and analyze the application status of hydrogel in skin wound treatment. Finally, we believe that the combination of AI and optical imaging technology in the development and efficacy monitoring of hydrogels will be a promising research direction in the future.

Keywords: hydrogel, OCT, *in vivo* imaging, artificial intelligence, wound healing

1. Introduction

As the largest organ system in the human body, the skin plays a vital role in maintaining the body's physiological stability, protecting the skin from external stimuli, preventing infection, and maintaining fluid balance. Therefore, skin wound healing is an important step in the survival to complete wound closure [1]. Although human skin can heal itself after injury, this is limited to superficial wounds. In cases such as deep burns or diabetes, the wound's self-healing ability is limited, and supportive methods are needed to accelerate and protect the wound healing process. Current conventional approaches to wound treatment including the application of different types of dressings, electrical stimulation therapy, skin grafting, and negative pressure wound therapy (NPWT) have proven beneficial, but they also have certain limitations [2].

Since O. Wichterle et al., reported the first case of hydrophilic gel in 1960, the results of the application of hydrogel in wound healing have become increasingly abundant [3–9]. More and more research results show that hydrogels have the ability to deliver drugs, cytokines, and growth factors as carriers, which will greatly accelerate wound healing. In addition, compared with traditional dressings, the non-adhesive nature of the hydrogel avoids secondary damage, and its 3D network structure is conducive to absorbing wound exudate while maintaining an ideal moist environment [10–13]. In view of this, hydrogels have gradually become ideal wound dressings in recent years and show good prospects in the treatment of burns and other skin injuries [14, 15]. In this chapter, we describe advanced hydrogels for wound healing and enhanced skin repair.

1.1 Development of injectable hydrogel

To date, a plethora of biomaterials as wound dressings for different clinical treatment protocols have been developed, which may be composed of synthetic or natural materials, or may be a hybrid of the two. Naturally occurring polymers, such as sodium alginate (SA), chitosan (CS), gelatin, and hyaluronic acid (HA), are biocompatible and biodegradable, which allow adhesion and coordination of cellular responses [16]. Unfortunately, natural hydrogels suffer from some limitations, such as not having strong mechanical properties and significant batch-to-batch variability [17]. In contrast, synthetic polymers such as polyvinyl alcohol (PVA), polyacrylamide (PAM), and polyethylene glycol (PEG) have become increasingly popular due to their strong mechanical properties, customizable structures and low immunogenicity [18]. However, the application of synthetic polymers in the field of biomedicine should pay attention to the rejection of the body. Therefore, more complex hydrogels were synthesized. Currently, the material design of hydrogels usually combines natural biopolymers and synthetic polymers to overcome the limitations brought by a single polymer [18]. Hydrogels are formed by cross-linking polymer chains dispersed in an aqueous medium, and the cross-linking methods mainly include physical entanglement, ionic interactions, and chemical cross-linking (**Figure 1**) [19]. Physical cross-linking is usually non-permanent, not as stable as chemical cross-linking, and has cross-linking reversibility, but it is sufficient for polymer chains to aggregate to form gel substances that are insoluble in aqueous media. Due to the covalent bonds between different polymer chains, chemically cross-linked gels have excellent mechanical strength because they are mainly connected by covalent bonds, but their preparation requires the addition of chemical initiators or cross-linking agents. It has been reported that the cross-linking agent has certain toxicity, so the cross-linking agent used to prepare the hydrogel should be extracted from the hydrogel before use, which increases the complexity of the use of chemically cross-linked gel [20]. Electron beam (EB) radiation cross-linking technology can overcome the above defects, which belongs to the grafting in chemical cross-linking and is more stable than the physical cross-linking network structure. Furthermore, when using radiation crosslinking, neither initiators nor crosslinking agents are required, making it safer, softer, and more stretchable than traditional chemical crosslinking [21]. Work in the late 1990s showed that hydrogel precursors can be injected via standard syringes without the need for pre-molding and the use of highly invasive surgical procedures to deliver the material to the target site. Injectable hydrogels have received increasing attention in recent years due to their excellent self-healing ability and minimal invasiveness [22]. Injectable hydrogel technology can better reproduce the complex extracellular

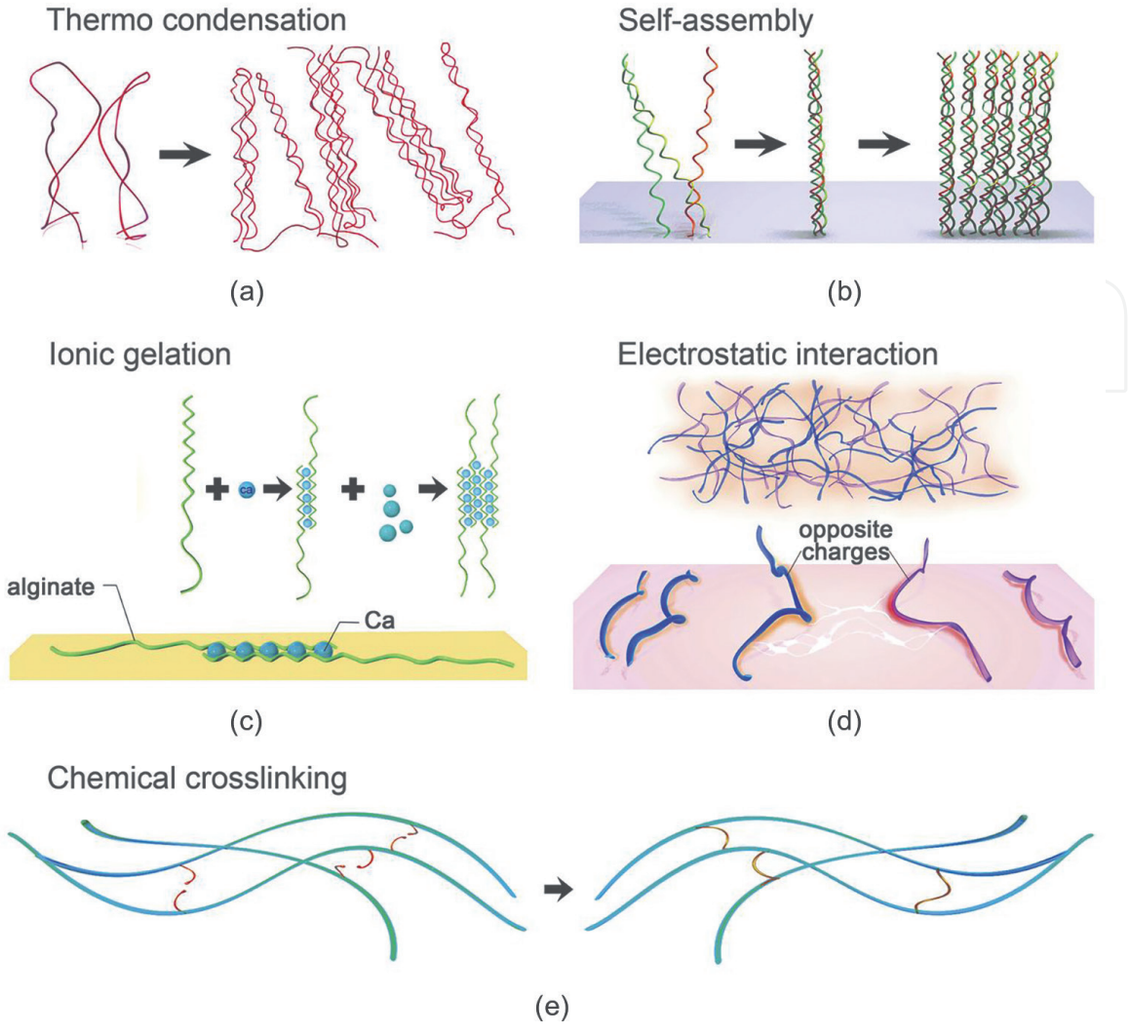

Figure 1.
Cross-linking of hydrogels. (a to d) physical cross-linking. (a) Thermally induced entanglement of polymer chains. (b) Molecular self-assembly. (c) Ionic gelation. (d) Electrostatic interaction. (e) Chemical cross-linking. Reprinted with permission from reference [19].

environment and maintain cell viability, thereby enabling adequate delivery of cells and therapeutic small molecules, which enables the development and optimization of novel therapeutic injectable Hydrogels [23, 24].

Gelatin is inexpensive and readily available and has good cell adhesion [25]. Alginates are commonly used in the treatment of deep second-degree burns due to their excellent biological properties, exudate absorption potential, and ability to maintain a moist wound environment [26–28]. In addition, carboxymethyl cellulose (CMC) contains a large number of carboxymethyl groups, which facilitates polymerization with other material [29, 30]. Their combined strengths make up for the deficiencies of one or both of these natural polymers for applications.

The EB radiation cross-linking mechanism in **Figure 2** is proposed for cross-linking of injectable 3D-PH. The radiation energy of EB is mainly absorbed by water in aqueous solution, and the radiation decomposition of water mainly produces reactive species such as hydroxyl radicals (OH) (**Figure 2a**) [32]. Amino acid residues in gelatin molecules are easily self-oxidized to form aldehyde groups, and aldehyde groups can cross-link with amino acids on gelatin molecules to form Schiff bases (**Figure 2b**), which is the first cross-linked network. Injectable 3D-PH

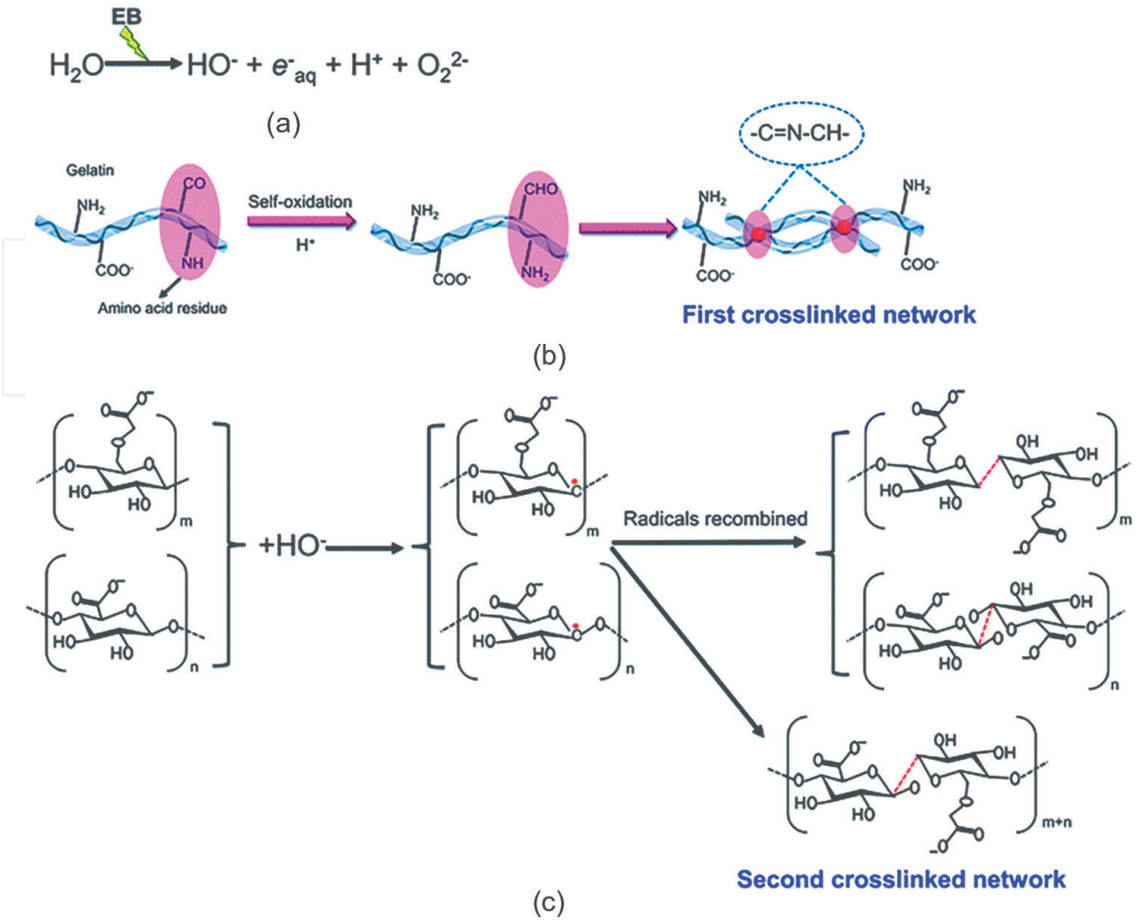

Figure 2.
Mechanism of EB radiation crosslinking of injectable 3D-PH. (a) Ionizing radiation reaction equation of water in polymer aqueous solution. (b) Gelatin self-crosslinking to form the fifirst network of injectable 3D-PH. (c) the crosslinking mechanism of alginate and CMC under EB irradiation. Reprinted with permission from reference [31].

Furthermore, OH- is considered to be a very reactive species, which can remove H from alginate and CMC carbon chains, inducing the formation of alginate-derived radicals, CMC-derived radicals, and HO. Subsequently, the radicals recombine to form new covalent bonds between the carbon chains (**Figure 2c**), which is a second cross-linked network. Hydrogen bonds formed between the injectable 3D-PH stabilize the chemical structure of the hydrogel. The new bonds formed during electron beam irradiation made the molecular chains of the hydrogel connect more tightly. The double-crosslinked network structure triggered by EB and Schiff base can significantly strengthen the hydrogel. These results demonstrate that EB irradiation cross-linking injectable 3D-PH can form a stable double-cross-linked network structure [31].

In view of this, our team designed an injectable 3D-PH via EB radiation crosslinking gelatin-alginate-carboxymethyl cellulose solution, which developed by green materials and facile applicable method (**Figure 3a**). In another study, Zhang et al. synthesized dopamine-modified gelatin@Ag nanoparticles (Gel-DA@Ag NPs) by chemical grafting for wound healing as shown in **Figure 3b** [33]. For the first time, they found that the biomineralization ability of gelatin can be enhanced with dopamine-modified gelatin (Gel-DA). This biomineralization-enhancing strategy provides a new strategy for developing organic and inorganic hybrid multifunctional

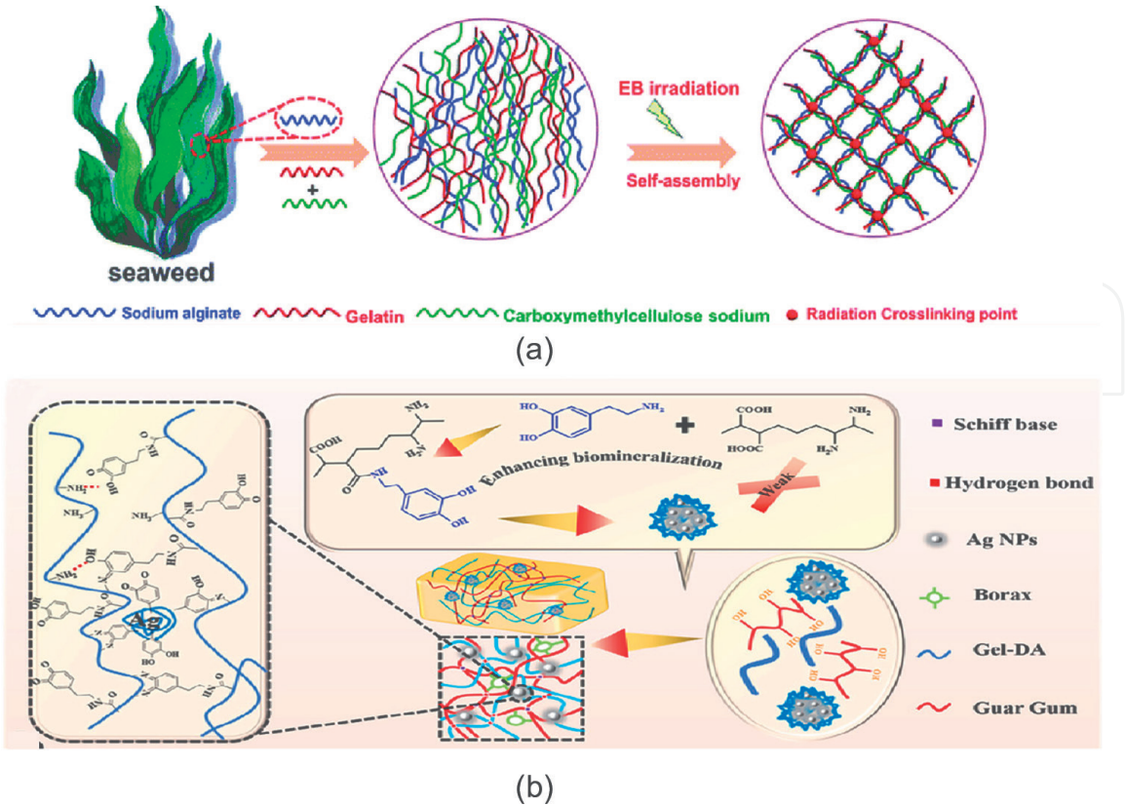

Figure 3.
Schematic diagram of the preparation of hydrogels. (a) 3D-PH. (b) Gel-DA/GG@Ag hydrogels. Reprinted with permission from reference [31, 33].

hydrogels. Among the two different materials, gelatin plays different roles, the former mainly induces platelet activation for wound hemostasis and the latter mainly acts as a biomineralizer combined with metal nanoparticles, resulting in different functional localization.

1.2 Design points of hydrogels for wound treatment

Given the characteristics of the wound surface, the goals of wound management seem obvious, including providing temporary wound coverage, preventing infection, and relieving scarring [34]. Because bacterial infection can hinder the regeneration of epithelial cells and the synthesis of collagen, the prevention of wound infection is an important function of wound dressings [35]. To achieve this function, some broad-spectrum antimicrobial agents are often added to hydrogels, such as silver ions/nanoparticles (AgNPs) [36]. Zhang et al. compared the antibacterial properties of Gel-DA/GG@Ag hydrogels by spread plate method using two hydrogels with only guar gum (GG) and without silver ions (Gel-DA hydrogel) as the control group. As shown in **Figure 4b**, in the three treatments, the number of bacterial colonies in the GG and Gel-DA hydrogel did not change significantly, but in the GG@Ag hydrogel treatment group, the number of colonies of *Escherichia coli* and *Staphylococcus aureus* was significantly reduced, reflecting the antibacterial effect of AgNPs." Guo et al. synthesized a hydrogel TS-Gel-Ag-col with antibacterial and anti-inflammatory functions for wound treatment, which was prepared by muco-mimetic poloxamer 407 (F-107), polyvinylpyrrolidone, and dencichine/chitosan dialdehyde synergistic cross-linked aggregated collagen nanofibers decorated with silver nanoparticles [37]. The

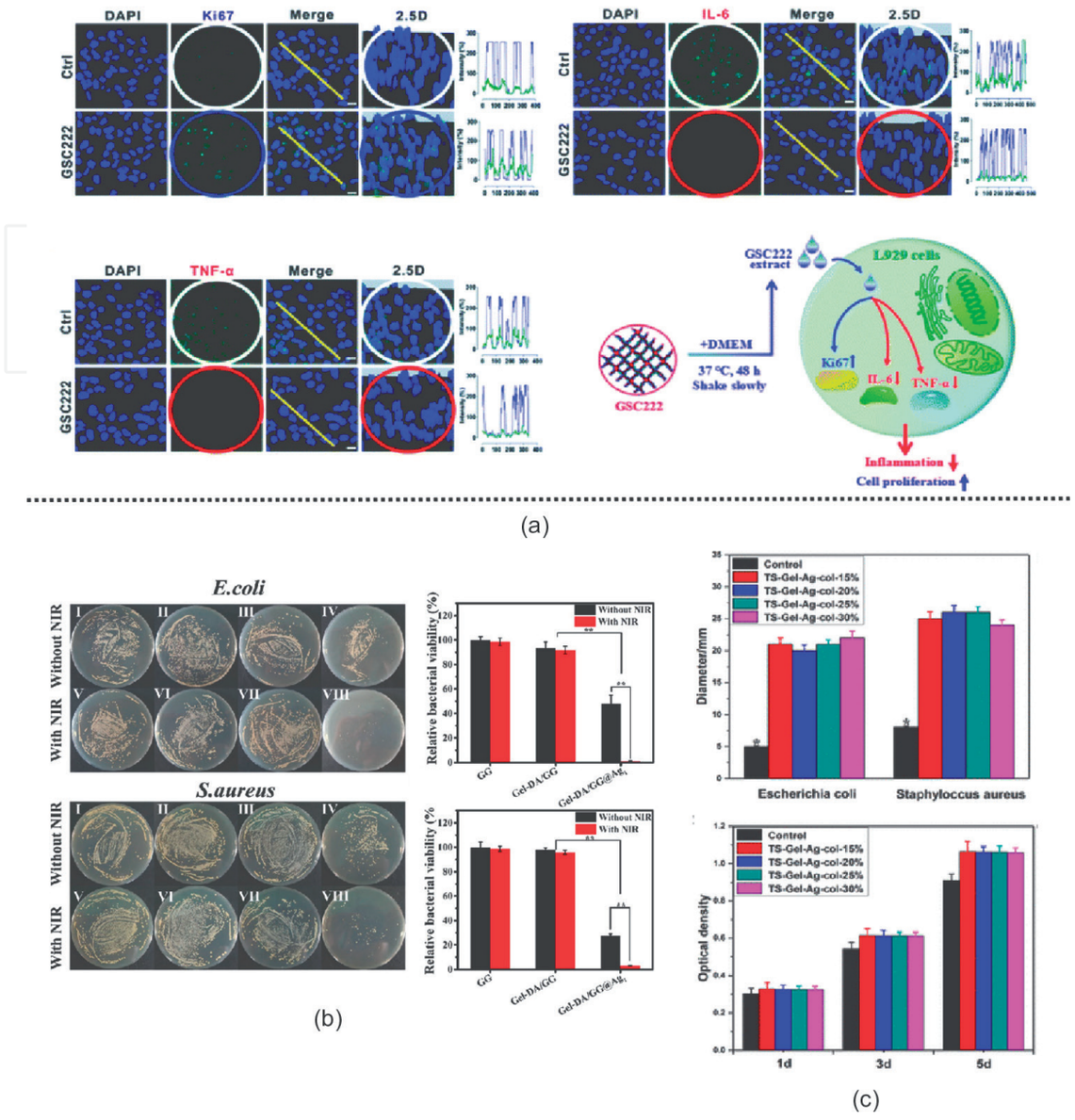

Figure 4.
Antibacterial and anti-inflammatory properties of hydrogels. (A) 3D-PH stimulate cell proliferation and suppresses inflammation in L929 cells. (B) Photographs of E. coli and S. aureus colonies after treatments and the relative survival rates with I) PBS, II) GG, III) gel-DA/GG, IV) gel-DA/GG@Ag1, V) PBS + NIR, VI) GG + NIR, VII) gel-DA/GG + NIR, and VIII) gel-DA/GG@Ag1 + NIR. Power density: 2 W cm^{-2}, 10 min. (C) Antimicrobial effect of TS-gel-Ag-col with different F-107 contents against E. coli and S. aureus and effect of F-107 contents on the proliferation of fibroblasts on TS-gel-Ag-col at different time intervals (1 d, 3 d, and 5 d). Reprinted with permission from reference [31, 33, 37].

addition of F-107 will make the hydrogel have a heat-reverse gelation and enhance biocompatibility, which can overcome the loss of the original native hierarchical aggregated structure present in living tissue fabricated by post-functionalization of collagen molecules [38, 39]. By comparing the inhibition zone diameters of *E. coli* and *S. aureus* affected by different types of gels, the authors found that the amount of F-107 had no significant effect on the bacteriostatic properties of TS-Gel-Ag-col. In addition, although TS-Gel-Ag-col without silver nanoparticles (AgNPs) also exhibited certain antibacterial properties due to the presence of dialdehyde chitosan, the antibacterial effect of AgNPs was more significant (**Figure 4c**). It can be seen that TS-Gel-Ag-col also enhanced the antibacterial effect of the hydrogel through AgNPs.

The high concentration of silver in this silver-containing hydrogel can provide a faster rate of bacterial inhibition, but at the same time cause cytotoxicity, and low concentrations have no significant cytotoxicity to cells, but the rate of inhibition is slow [40]. Therefore, when designing wound dressings, the silver content in the hydrogel needs to be carefully considered to achieve the optimal balance between low cytotoxicity and high antibacterial activity. However, given the oxidative damage and potential toxicity of silver nanoparticles in tissues, researchers prefer to directly synthesize hydrogels from materials with antibacterial properties rather than adding antibacterial agents [41–43].

The occurrence of inflammation is the basis of wound healing, but excessive expression of inflammatory mediators will cause some cells and tissues to atrophy and form chronic inflammation, thereby impairing the healing of skin wounds [44]. Therefore, the anti-inflammatory functional design of hydrogels is equally important. To investigate whether 3D-PH can block inflammatory signaling activation and promote cell proliferation, we used confocal laser scanning microscopy to quantify the expression of cell proliferation-related protein Ki-67 and inflammatory factors (IL- 6, TNF-α, etc.).The results showed that injectable 3D-PH successfully blocked inflammatory signaling activation and stimulated dermal fibroblast proliferation and migration in vitro (**Figure 4a**). Specifically, the level of Ki-67 was increased, while the expression of inflammatory factors was decreased. All of these are beneficial to accelerate the healing process of deep second-degree burn wounds in vivo [31].

Scars often appear after an injury, and scarring of various types can have long-term psychological and physical effects on patients, especially those located in frequently exposed areas [45]. Therefore, scar management is also an important part of wound management, and the ideal result is a dressing that minimizes scarring while allowing the wound to heal quickly. Injectable 3D-PH has the ability to accelerate necrotic tissue removal and wound healing [31]. As shown in **Figure 5a**, the injectable 3D-PH, coloplast wound dressing and blank control were injected into the wounds of second-degree scald. The results showed that after 20 days of treatment, the wounds treated with 3D-PH injection were almost invisible, and the healing rate was significantly higher than the other two groups (**Figure 5b**). Two other hydrogels, Gel-DA@AgNPs and TS-Gel-Ag-col, also have great potential to repair skin tissue (**Figure 5c** and **d**). The researchers used a mouse full-thickness Staphylococcus aureus-infected wound model to demonstrate the properties of Gel-DA@Ag in promoting wound healing. It can be seen that among the groups, the gel DA/GG@Ag1 + NIR group had the best wound regeneration effect, showing an advantage on the fourth day of treatment, and significant epidermal regeneration could be observed, proving that Gel-DA/GG @Ag has the effect of intrinsically accelerating wound healing [33]. **Figure 5d** shows three types of traumatic bleeding models were synthetically utilized to evaluate the hemostatic performance of TS-Gel-Ag-col *in vivo* [37]. The results clearly showed that TS-Gel-Ag-col presented significantly faster hemostasis as compared to the commercial Helitene collagen hemostatic material. And due to the injectable nature of these two hydrogels, when a sol–gel transition occurs, the wound can be easily covered comprehensively and fit well to the injury site. In addition, the 3D porous structure of the hydrogel is important for wound healing, because the denseness of the porous material can prevent the escape of red blood cells and platelets. At the same time, the presence of hydrophilic residues in the 3D grid of the hydrogel enables the hydrogel to further absorb wound exudate and provide a hypoxic and humid healing environment, shortening the healing time of the epidermis [46, 47].

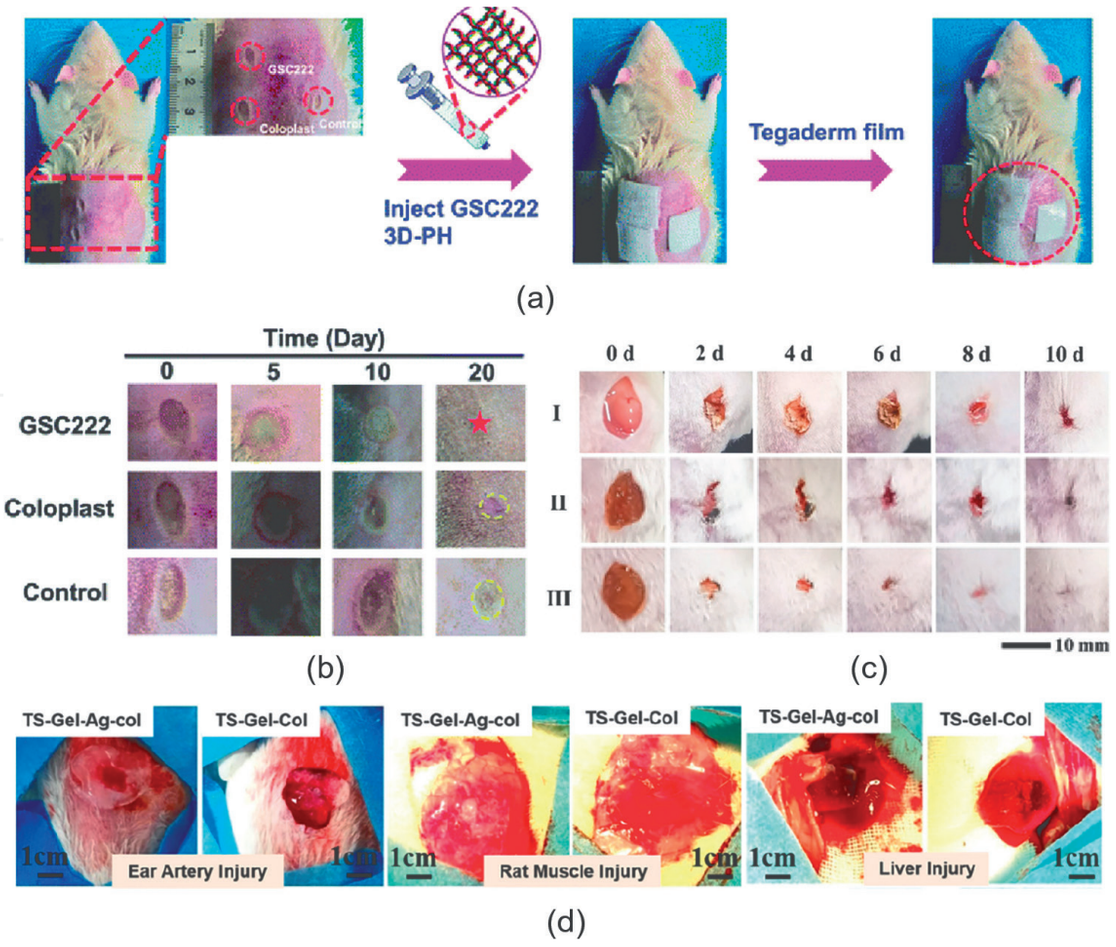

Figure 5.
Healing of animal wounds treated with hydrogels. (a) schematic diagram of the surgical procedure. (b) Coloplast wound dressing, 3D-PH, and control group recovery of scalded wounds in rats on days 0, 5, 10, and 20. (c) Photographs of S. aureus-infected wounds with different treatments. I) Control, II) gel-DA/GG@Ag1, and III) gel-DA/GG@Ag1 + NIR. (d) Photographs of rat muscle trauma, liver and rabbit ear artery injury after TS-gel-Ag-col and TS-gel-col treatment. Reprinted with permission from reference [31, 33, 37].

Most importantly, the 3D porous network structure of the hydrogel resembles the natural extracellular matrix, which will facilitate the adhesion of cells, tissue factors and growth factors for delivery [24].

2. Optical technology applying on the skin *in vivo*

Histology remains the most accurate method for wound healing assessment, including biopsy and chamber-embedding, re-epithelization, epithelial thickness index, granulation tissue thickness, remodeling, and scarring can be obtained by histological analysis. Moreover, visual inspection also can evaluate woundswhich is based on observations such as wound size, color, odor, and level of pain [48–51]. The limitations of the histological analysis method are mainly invasive and destructive, the method generates new wounds during the examination, which delays the time of wound healing and is not suitable for patients at high risk of wound infection, thus reducing the accuracy of wound assessment. Therefore, non-invasive monitoring techniques are a safer way to assess and monitor wound healing, which can help clinicians and researchers more objectively determine and assess whether healing is

improving or deteriorating [50–52]. DRS is a non-invasive technique, and the general configuration of a DRS system includes a light source, a photodetector, and a fiber optic probe for light transmission. The DRS can measure the characteristic diffuse reflectance spectrum of tissue in the visible to near-infrared wavelength range. The tissue structure was restored by diffuse reflectance using photon transmission model and least squares curve fitting algorithm. In addition, DRS can also obtain information such as chromophore concentration, absorption and scattering properties of tissues such as breast and skin [53–55]. OCT provides a non-invasive method for obtaining optical cross-sections of the superficial cortex [56, 57], which uses the light scattering characteristics of tissue to construct high-resolution subsurface images. OCT is based on the same echolocation principle as an ultrasound but uses light waves instead of acoustic waves. **Figure 6** shows schematic diagram of the DRS and OCT system.

2.1 Evaluation of skin scars and structure by DRS

Hsu, Chao-Kai et al. assessed the severity of scarring by measuring the diffuse reflectance of the skin. **Figure 7a** shows the representative clinical pictures of keloid (KS, black solid circle) and normal scars (NS, red solid circle) of one of such patients. The uninjured skin located 3 cm away from the keloid (CKS, black dashed circle) and normal scars (CNS, red dashed circle) were used as control groups. It can be seen that in the range of 500–600 nm, the absorption rate of keloids is higher than that of normal scars and uninjured skin, and the magnitude of the reduced scattering spectrum of keloids is the lowest (**Figure 6b** and **c**) [53]. The results of this study demonstrate that the DRS system can not only quantify collagen concentration, water content,

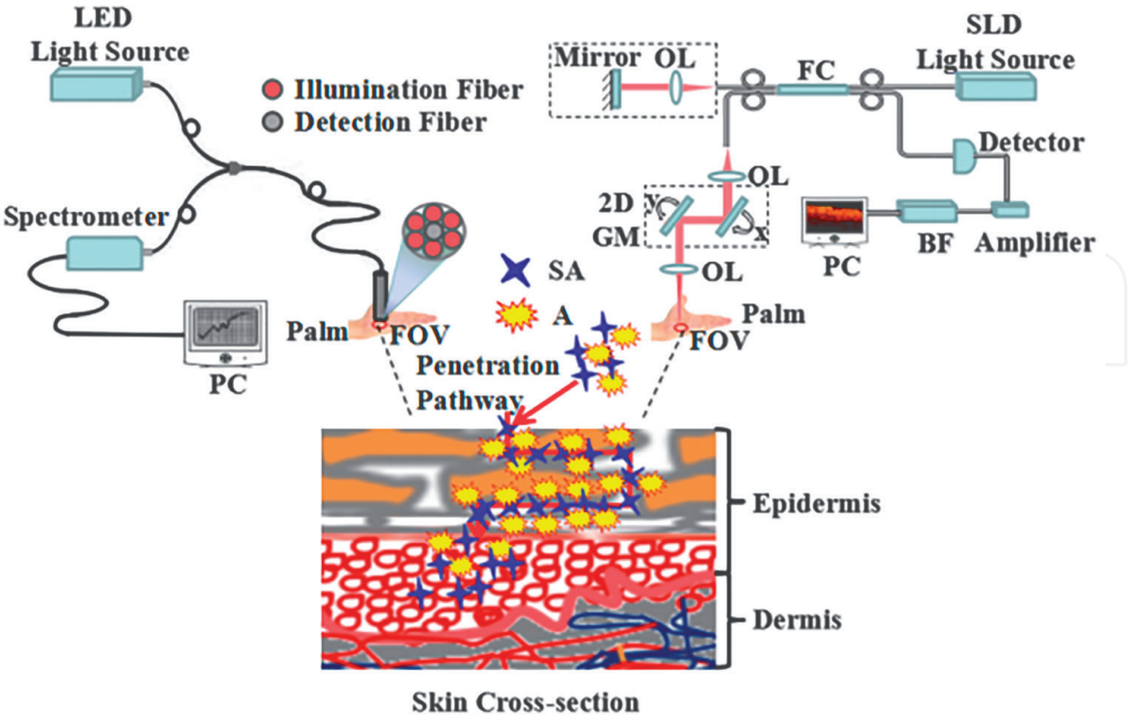

Figure 6.
Schematic diagram of the DRS and OCT system. SLD: Super-luminescent diodes, FC: Fiber coupler, GM: Galvo mirrors, OL: Objective lens, PC: Personal computer, BF: Bandpass filter, FOV: Field of view, SA: Salicylic acid, a: Azone. Reprinted with permission from reference [58].

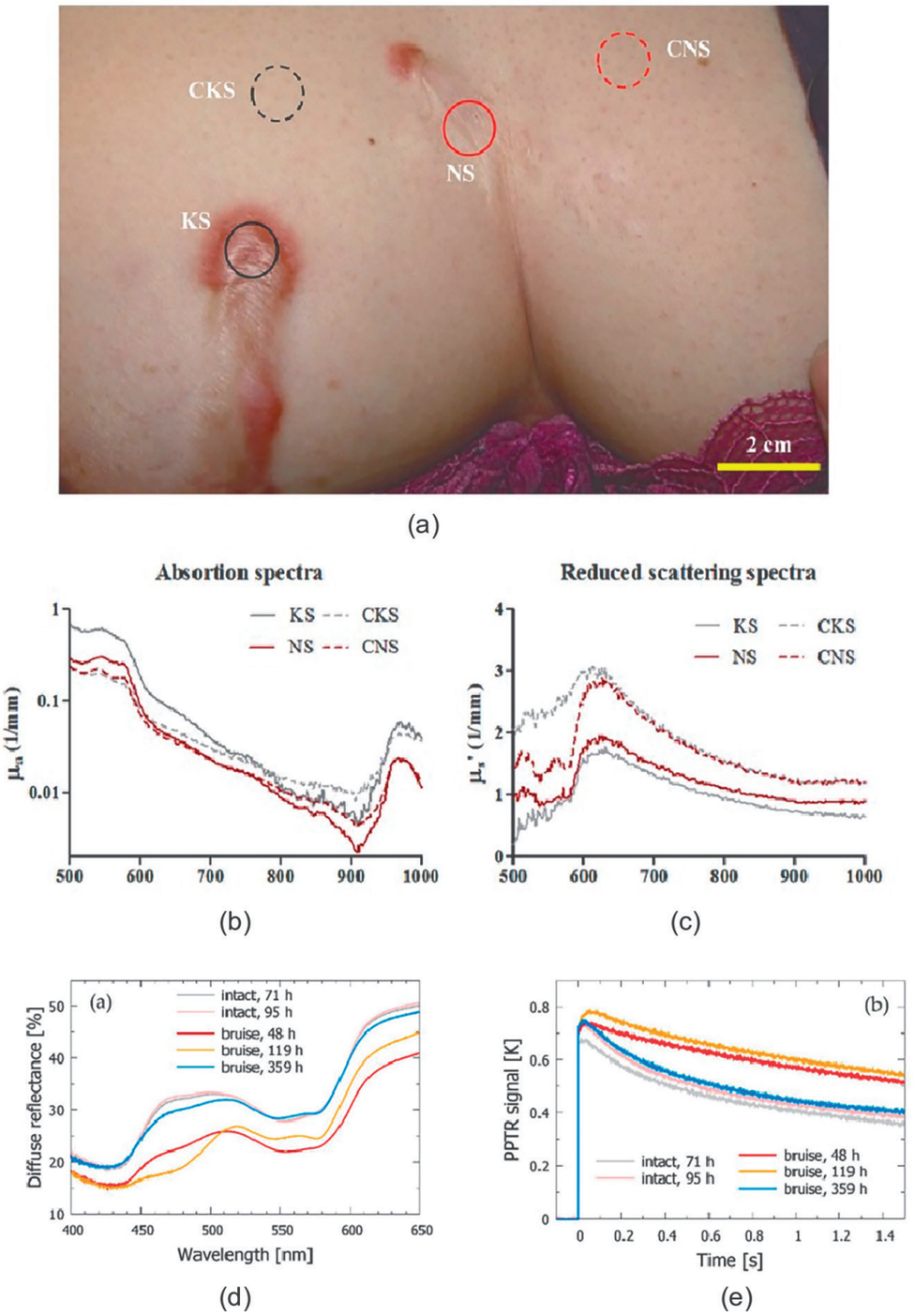

Figure 7.
(a) The clinical picture of a keloid patient containing keloid scar (KS), normal scar (NS)the uninjured skin (CKS), and normal scars (CNS). (b) Typical absorption and (c) reduced scattering spectra in KS, NS, CNS and CKS, (d) DRS spectrum and (f) PPTR signal as obtained from the intact skin site near the bruise in subject a (solid orange curves) and the best-fitting model predictions (dashed lines). Reprinted with permission from reference [53, 59].

and oxygen saturation, but also determine the alignment of collagen bundles in keloid scars. In another study, Bin Chen et al. developed a DRS-based inverse method to extract structural parameters of skin tissue. The model was experimentally validated by constructing a skin model and performing spectral measurements, which

demonstrated the agreement between the measured and calculated spectral data [60]. Marin, Ana et al. combined diffuse reflectance spectroscopy and pulsed photothermal radiometry (PPTR) in the visible spectral range to examine the dynamic process of traumatic bruising recovery, while using a numerical model of light and heat transport in a four-layer model of human skin from data for both techniques. **Figure 6d** and **f** shows both DRS spectra and PPTR signals obtained from the bruised site display large differences with respect to the nearby intact site.We can see a significant reduction in diffuse reflectance can be seen throughout the presented spectral range, mainly due to the higher blood content in the dermis [59]. These tasks show that DRS should also be able to quantitatively evaluate the wound healing during the treatment of wounding gel, including the scar condition after wound healing, whether the wound ulcers occurs.

2.2 Investigating the wound healing by OCT and OMAG

In recent years, how to extract the blood flow information in tissue capillaries and image the microcirculation blood flow of tissue capillaries has become a hotspot in the field of OCT research. Compared with OCT, OCT microangiography (OMAG) is a novel technique that can provide microcirculatory imaging enabled by processing OCT data [61].

For this reason, OCT technology has been extended to develop OMAG. OMAG uses the structural imaging of OCT to extract tissue blood flow information through algorithms, so as to achieve non-invasive, non-contact, and no need for contrast agents to image blood flow in tissue capillaries [62, 63]. Wang et al. [64] used an imaging system that combined dual wavelength laser speckle imaging (DW-LSI) with DOMAG to image the ears of mouse, which monitored hemodynamic changes during acute wound healing. After the wound was created using the biopsy punch, the blood flow in the first-order branches of the affected arteries and veins in the laser speckle image was markedly reduced as can be seen from the orange circles in **Figure 8B**. In addition, detailed changes in axial blood flow velocity can be found in the DOMAG image (**Figure 8C**). 10 min after perforation, compared with the baseline image at the white circle in **Figure 8C** (b), the two venous branches of the involved vessel and its downstream disappeared. At the same time, the left collateral vein was significantly increased to compensate for blood flow (white arrows in **Figure 8C** (b). Finally, changes in blood flow were quantified by integrating the flow velocity in the projection plane to obtain arterial flow maps.

Furthermore, blood vessel images can be obtained by incorporating OMAG technique into PS-OCT instrument [65]. Both Jung-Taek Oh and Kwan S Park used PS-OCT for quantitative assessment and monitoring of wound healing. Epidermis (E) and dermis layers (D), blood vessel (V), and cartilage (C) in the tissue of the pinna is observable in the reflectivity images. And blood vessels can be separately visualized in the blood vessel images by OMAG technique (**Figure 8D**) [65, 66]. The phase retardation image represents cumulative phase retardation due to the birefringence inside the tissue because the difference in phase shift between two characteristic polarization states of backscattered light from the tissue is altered by the tissue birefringence. Therefore, PS-OCT can characterize the amount of collagen by measuring the polarization parameters of the sample, such as phase retardation and degree of polarization (DOP), which will help us to observe the growth direction and recovery of the wound [67].

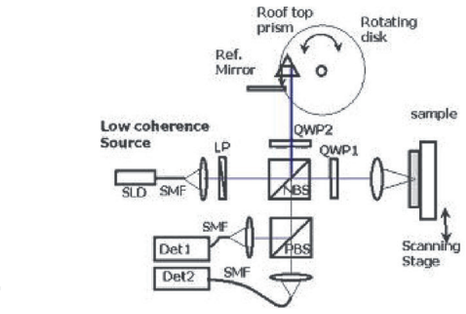

(a)

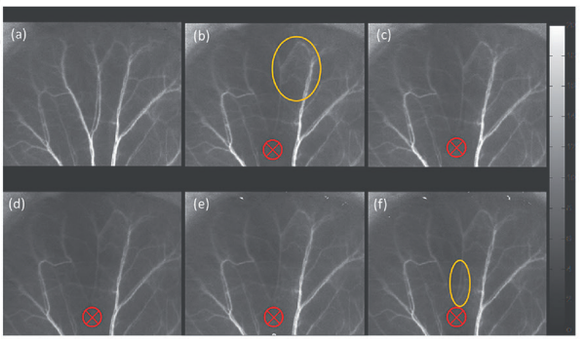

(b)

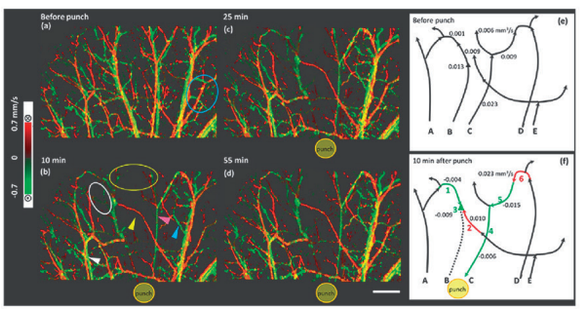

(c)

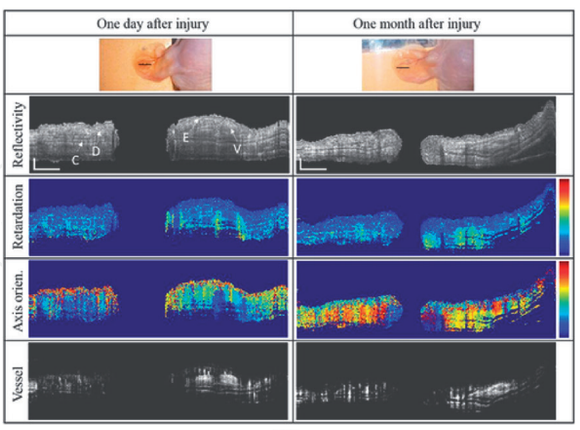

(d)

Figure 8.
(a) Schematic of the bulk-type PS-OCT system. (b) Images acquired from the laser speckle imaging system showing the large-scale blood flow changes of the mouse ear following a punch biopsy. (a) Baseline image of the mouse ear before punch; (b)-(f) are images taken at 10 s, 5 min, 10 min, 25 min, and 55 min after punch, respectively. Scale bar: 1 mm. (c) Changes in blood flow velocity and direction of the mouse ear following a punch biopsy. (a) Baseline DOMAG image of the mouse ear; (b), (c) and (d) are DOMAG images taken at before punch, 10 min, 25 min and 55 min after the punch, respectively. (e) and (f) are skeletonized arterial network at baseline and at 10 min after he punch, respectively. 1–6 denote the blood vessel segments that have shown significant blood flow changes, A-E denote the five main arterial branches. Scale bar: 1 mm. (D) Multifunctional PS-OCT imaging of the punch biopsy wound model of a mouse. Reprinted with permission from reference [64–66].

3. AI for extracting and quantitating the feature information of skin

Artificial intelligence (AI) came out in 1956. This technology is widely used in various fields, and realizes intelligent diagnosis and treatment in the medical field through the screening, diagnosis, and management of diseases. Machine learning (ML), which is a subset of artificial intelligence, is represented by mathematical algorithms that improve learning through experience. There are two main types of machine learning algorithms (**Figure 9**): (i) unsupervised (ability to spot patterns), (ii) supervised (classification and prediction algorithms based on previous examples) [68–70]. ML has gradually become a common method for solving difficult problems in artificial intelligence because computer algorithms can be automatically improved through previous experience [71]. There are dozens of algorithms in ML, including deep learning, decision trees, clustering, and Bayesian. For example, the use of decision trees to monitor the depth of anesthesia is a type of ML [72]. Artificial neural networks (ANNs) are mathematical models of information processing based on structures similar to the brain's synaptic connections. ANNs have performances such as self-learning, associative storage, and fast finding optimal solutions, which are far superior to ML algorithms, and are especially suitable for dealing with cluttered and unstructured data (such as images, audio, and text) [73]. As researchers delved into the structure of ANNs, Deep neural networks (DNN) with more and more complex network hierarchies were produced [74]. It also means that DNNs are more capable of modeling or abstract representations of things, as well as simulating more complex models.

3.1 Supervised learning for dermatology

Skin cancer is a common cancer type [75]. Melanoma and non-melanoma are the two main types of skin cancer, with melanoma being the most dangerous type of skin cancer with a high mortality rate [76]. Traditional methods for early detection of skin cancer include skin self-examination and skin clinical examination [77]. However, skin self-examination is a random method and its accuracy depends on how well people know about skin cancer. In addition, the use of professional medical tools such as dermoscopy and microspectroscopy for clinical examinations is not only expensive but also requires professionals to operate [78]. Therefore, using AI to identify patients and upload shared images for diagnosis has become a more convenient method.

The most commonly used machine learning algorithm in dermatology is supervised learning. It is mainly related to retrieval-based AI, where we need to input already labeled data in advance [79]. The goal is to analyze this training data and produce an inferred feature that can be used to map out new instances. For example, when identifying benign and malignant skin lesions, we need to label the skin lesions images as benign and malignant in advance. In this approach, automatic classification of new and unlabeled images can be achieved once training on these images is complete. Esteva et al. explored the accuracy of this skin cancer classification algorithm by comparing deep-learning diagnoses with labeled results from 21 dermatologists. They used approximately 1.28 million images (1000 object categories) from the 2014 ImageNet Large-Scale Visual Recognition Challenge as pre-training objects to form validation and testing datasets. **Figure 10** shows the working system. The area under the curve (AUC) of the CNN algorithm exceeds 91%, indicating that the sensitivity and specificity in the classification of epidermal and melanocytic lesions is superior to

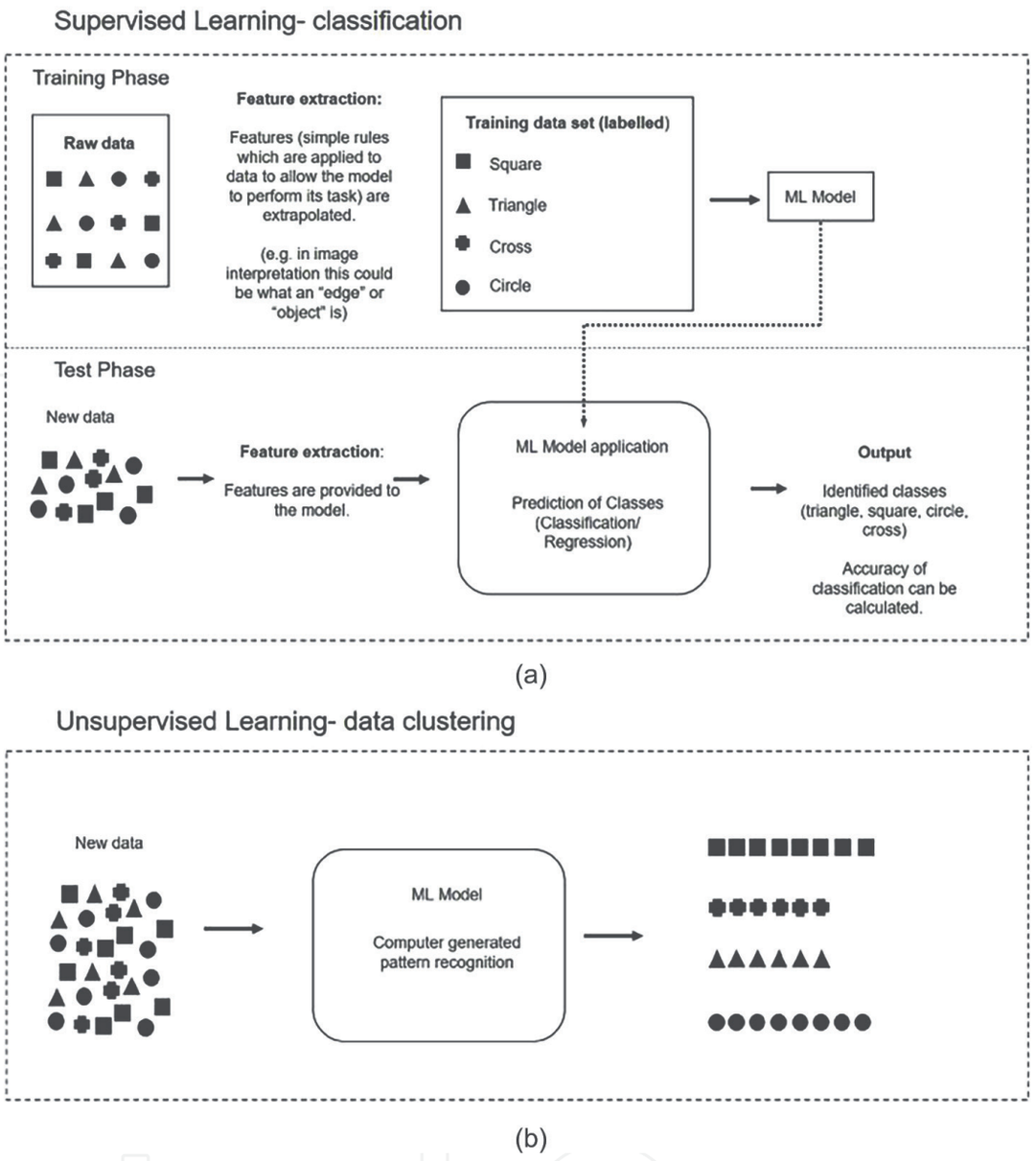

Figure 9.
Machine learning algorithms (a) supervised learning (b) unsupervised learning. Reprinted with permission from reference [68].

that of dermatologists. The results of this study show that, well-trained deep learning enables highly accurate diagnostic classification [80]. At present, ML has been gradually applied in combination with optical technology, which is mainly manifested in the use of AI-assisted analysis of OCTA data to achieve advanced diagnosis and correction of dispersion problems in OCT images to improve axial resolutio [81, 82]. These findings will help advance the application of AI in wound healing monitoring.

3.2 Unsupervised learning for dermatology

Unsupervised learning means that the algorithm is only given input data without corresponding output values. This type of algorithm is more of an exploration and does not have the correct output value [83]. Therefore, unsupervised methods are often suitable for situations where the statistics vary widely. For example, in a study

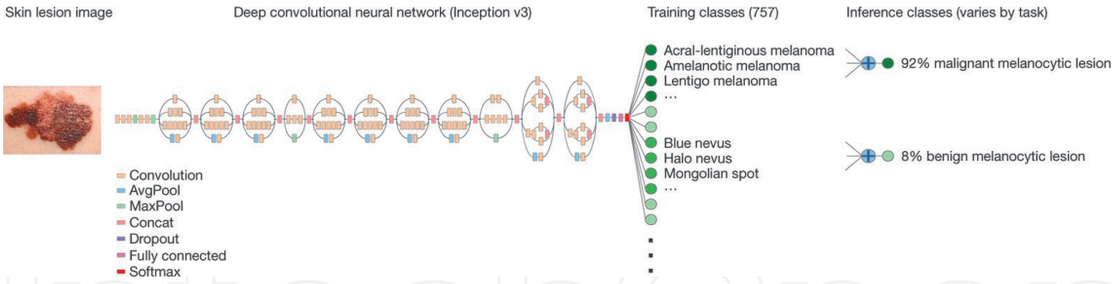

Figure 10.
Deep CNN layout. Reprinted with permission from reference [80].

by Kharazmi et al. [84] detecting basal cell carcinoma (BCC), unsupervised learning was used to classify vascular features in BCC dermoscopy for automatic cancer detection. The results show that the framework outperforms the state-of-the-art norm supervised learning results by 7% in Area Under Curve (AUC), with a sensitivity of 98.1% for BBC detection. This approach eliminates the need for supervised learning to use large and dense datasets at multiple scales to find appropriate images to build blocks of visual content [85]. So the advantage over supervised learning is that the algorithm is free to act in order to learn more about the data and present interesting findings. It is popular in clustering applications or the behavior of discovering groups in data and associations or predicting the behavior of rules that describe data.

3.3 Deep learning for classification of OCT images

OCT is also often used to detect BBC at the dermis-epidermal junction due to its ability to sub-epidermally visualize the skin structure and any underlying lesions [86]. Li et al. [87] used an image-based approach to identify the skin surface and normalized the skin image by surface flattening, then used pre-trained AlexNet, VGG-16, VGG-19 and GoogLeNet for deep feature extraction, and finally used SVM for BCC Classification. The experimental results show that the system based on the VGG-16 image descriptor is the best with a sensitivity of 0.935.

In the current research, image-based deep learning is mainly used in medical image noise reduction and reconstruction processing. Disease diagnosis mainly focuses on tumor detection, brain nervous system disease classification, and cardiovascular disease detection. There are few related studies in the field of skin [88–93]. For example, Kermany D et al. applied deep learning to a dataset of optical coherence tomography images to form a diagnostic tool for screening patients with common treatable blind retinal diseases. The trial results showed that the diagnostic tool was as accurate as hospital specialists in classifying age-related macular degeneration and diabetic macular edema [94]. Abdolmanafi et al. also used intra-coronary tomography images provided by intravascular optical coherence tomography (IV-OCT) as a deep learning library, and extracted the features of convolutional neural network features and fully convolutional network. The accuracy of the diagnostic models can be as high as 90% [95].

4. Challenges and perspectives

In conclusion, most current studies consider hydrogels to be ideal candidates for synthetic wound dressings because of their 3D structure and high water content

similar to skin, which ensures a moist environment for wounds [96, 97]. A wide variety of polymers have been used alone or in blends to create hydrogels designed for biomedical applications, with a focus on wound healing and less scarring [98–101]. In addition, most of the current research shows that non-invasive optical technology DRS and OCT may be useful for research related to abnormal wound healing. Although artificial intelligence has only realized the diagnosis of skin diseases [49, 52–55, 102], it will be gradually applied to the management of wound healing in the future.

Although the application of multifunctional composite hydrogels has obvious advantages, most of them are in the basic research stage of animal experiments, and there is still a lack of large-scale clinical studies to prove their efficacy and safety. In order to prevent and reduce the occurrence of adverse reactions, the indications and correct operation methods of each material hydrogel should be strictly mastered, and a comprehensive analysis of individuals should be carried out to remove adverse factors. We still have a long way to go in clinical application of wounds [103].

Dayong Yang et al. prepared persistent luminescent nanoparticles (PLNPs) containing a hydrogel (PL-gel) for targeted, sustained, and autofluorescence-free tumor metastasis imaging [104]. Professor Yu Lin's team develop a tri-modal bioimaging technique, they longitudinally and non-invasively track the degradation behavior of materials by designing and synthesizing thermosensitive hydrogels containing macromolecular fluorescent probes and magnetic resonance imaging (MRI) contrast agents, utilizing the collaborative application of optical techniques such as ultrasound, fluorescence, and MRI [105]. At present, the combination of hydrogel and optical technology mainly focuses on the tracking function. There are relatively few studies on the monitoring function of hydrogel in vivo efficacy, and there is still a lot of room for improvement.

The past few years have witnessed many changes in the fields of ML and Computer Science. Following this long progress, one may see many exciting developments in the next few years, but there are challenges before it can become more robust and be widely adopted in the clinic. AI is constrained by a lack of high quality, high volume, longitudinal, outcomes data [106]. Even the same image modality on the same disease site, the parameters of the imaging setting and protocols might be different in different clinical settings [91, 107]. But we believe that AI can play an important role in medical imaging and disease diagnosis when we master how to organize and preprocess data generated from different institutions and can encourage more sharing of image data.

Although there are relatively few studies on the use of deep learning in skin OCT and DRS imaging, current research on disease diagnosis systems combining AI and OCT leads us to believe that optical technology can be fully integrated with AI for wound healing monitoring [108]. This not only helps us to better detect the recovery of wounds treated with hydrogel dressings, but also more accurately evaluate the effectiveness of hydrogel treatment. In addition, AI based on optical images also helps to determine the type and depth of wounds, and can better design corresponding hydrogel wound dressings. Finally, we also believe that more and more new and safe wound dressings will be developed and applied with the aid of AI and optical imaging technology.

Acknowledgments and funding

This work was supported by the Natural science Foundation of Guangdong Province (2021A1515011654), Fundamental Research Funds for the Central

Universities of China (20720210117), Joint Funds for the Innovation of Science and Technology of Fujian province (2019Y9128), Xiamen Key Laboratory of Endocrine-Related Cancer Precision Medicine (XKLEC2021KF03, XKLEC2020KF04). Key Laboratory of OptoElectronic Science and Technology for Medicine of Ministry of Education, Fujian Provincial Key Laboratory of Photonics Technology (JYG2105). XMU Undergraduate Innovation and Entrepreneurship Training Programs (202210384051S202210384404, 2021X1119, 2021Y1119, S202110384391), and Shenzhen Bay Laboratory (SZBL2019062801005).

Conflict of interest

The authors declare that they have no known competing financial interests or personal relationships that could have appeared to influence the work reported in this paper.

Author details

Qingliang Zhao* and Lin Chen
Department of Laboratory Medicine, Shenzhen Research Institute of Xiamen University, Xiamen University, State Key Laboratory of Molecular Vaccinology and Molecular Diagnostics, Center for Molecular Imaging and Translational Medicine, School of Public Health, Xiamen, China

*Address all correspondence to: zhaoql@xmu.edu.cn

References

[1] Sorg H, Tilkorn DJ, Hager S, Hauser J, Mirastschijski U. Skin wound healing: An update on the current knowledge and concepts. European Surgical Research. 2017;**58**(1-2):81-94. DOI: 10.1159/000454919

[2] Hassanshahi A, Hassanshahi M, Khabbazi S, Hosseini-Khah Z, Peymanfar Y, Ghalamkari S, et al. Adipose-derived stem cells for wound healing. Journal of Cellular Physiology. 2019;**234**(6):7903-7914. DOI: 10.1002/jcp.27922

[3] Wichterle O, Lím D. Hydrophilic gels for biological use. Nature. 1960;**185**:117-118. DOI: 10.1038/185117a0

[4] Boucard N, Viton C, Agay D, Mari E, Roger T, Chancerelle Y, et al. The use of physical hydrogels of chitosan for skin regeneration following third-degree burns. Biomaterials. 2007;**28**(24):3478-3488. DOI: 10.1016/j.biomaterials.2007.04.021

[5] Kirker KR, Luo Y, Nielson JH, Shelby J, Prestwich GD. Glycosaminoglycan hydrogel films as bio-interactive dressings for wound healing. Biomaterials. 2002;**23**(17):3661-3671. DOI: 10.1016/s0142-9612(02)00100-x

[6] Balakrishnan B, Mohanty M, Umashankar PR, Jayakrishnan A. Evaluation of an in situ forming hydrogel wound dressing based on oxidized alginate and gelatin. Biomaterials. 2005;**26**(32):6335-6342. DOI: 10.1016/j.biomaterials.2005.04.012

[7] Griffin DR, Weaver WM, Scumpia PO, Di Carlo D, Segura T. Accelerated wound healing by injectable microporous gel scaffolds assembled from annealed building blocks. Nature Materials. 2015;**14**(7):737-744. DOI: 10.1038/nmat4294

[8] Cheng B, Yan Y, Qi J, Deng L, Shao ZW, Zhang KQ, Li B, Sun Z, Li X. Cooperative assembly of a peptide Gelator and silk fibroin afford an injectable hydrogel for tissue engineering. ACS Applied Materials & Interfaces 2018;**10**(15):12474-12484. DOI: 10.1021/acsami.8b01725

[9] Qu J, Zhao X, Liang Y, Zhang T, Ma PX, Guo B. Antibacterial adhesive injectable hydrogels with rapid self-healing, extensibility and compressibility as wound dressing for joints skin wound healing. Biomaterials. 2018;**183**:185-199. DOI: 10.1016/j.biomaterials.2018.08.044

[10] Kiyozumi T, Kanatani Y, Ishihara M, Saitoh D, Shimizu J, Yura H, et al. Medium (DMEM/F12)-containing chitosan hydrogel as adhesive and dressing in autologous skin grafts and accelerator in the healing process. Journal of Biomedical Materials Research. Part B, Applied Biomaterials. 2006;**79**(1):129-136. DOI: 10.1002/jbm.b.30522

[11] Jones AM, Vaughan DE. Hydrogel dressings in the management of a variety of wound types: A review. Journal of Orthopaedic Nursing. 2005;**9**(4):234-238. DOI: 10.1159/000085725

[12] Gennari O, Rega R, Mugnano M. A skin-over-liquid platform with compliant microbumps actuated by pyro-EHD pressure. NPG Asia Materials. 2019;**11**(1):1-8. DOI: 10.1038/s41427-018-0100-z

[13] Caló E, Khutoryanskiy VV. Biomedical applications of hydrogels: A review of patents and commercial

products - ScienceDirect. European Polymer Journal. 2015;**65**:252-267. DOI: 10.1016/j.eurpolymj.2014.11.024

[14] Li Z, Zhou F, Li Z, Lin S, Chen L, Liu L, et al. Hydrogel cross-linked with dynamic covalent bonding and Micellization for promoting burn wound healing. ACS Applied Materials & Interfaces. 2018;**10**(30):25194-25202. DOI: 10.1021/acsami.8b08165

[15] Sun G, Zhang X, Shen YI, Sebastian R, Dickinson LE, Fox-Talbot K, et al. Dextran hydrogel scaffolds enhance angiogenic responses and promote complete skin regeneration during burn wound healing. Proceedings of the National Academy of Sciences of the United States of America. 2011;**108**(52):20976-20981. DOI: 10.1073/pnas.1115973108

[16] Boateng J, Catanzano O. Advanced therapeutic dressings for effective wound healing--a review. Journal of Pharmaceutical Sciences. 2015;**104**(11):3653-3680. DOI: 10.1002/jps.24610

[17] Catoira MC, Fusaro L, Di Francesco D, Ramella M, Boccafoschi F. Overview of natural hydrogels for regenerative medicine applications. Journal of Materials Science. Materials in Medicine. 2019;**30**(10):115. DOI: 10.1007/s10856-019-6318-7

[18] Dimatteo R, Darling NJ, Segura T. In situ forming injectable hydrogels for drug delivery and wound repair. Advanced Drug Delivery Reviews. 2018;**127**:167-184. DOI: 10.1016/j.addr.2018.03.007

[19] Zhang YS, Khademhosseini A. Advances in engineering hydrogels. Science. 2017;**356**(6337):eaaf3627. DOI: 10.1126/science.aaf3627

[20] Patenaude M, Smeets NM, Hoare T. Designing injectable, covalently cross-linked hydrogels for biomedical applications. Macromolecular Rapid Communications. 2014;**35**(6):598-617. DOI: 10.1002/marc. 201300818

[21] Lu L, Yuan S, Wang J, Shen Y, Deng S, Xie L, et al. The formation mechanism of hydrogels. Current Stem Cell Research & Therapy. 2018;**13**(7):490-496. DOI: 10.2174/1574888X12666170612102706

[22] Mo C, Xiang L, Chen Y. Advances in injectable and self-healing polysaccharide hydrogel based on the Schiff Base reaction. Macromolecular Rapid Communications. 2021;**42**(10):e2100025. DOI: 10.1002/marc.202100025

[23] Elisseeff J, Anseth K, Sims D, McIntosh W, Randolph M, Langer R. Transdermal photopolymerization for minimally invasive implantation. Proceedings of the National Academy of Sciences of the United States of America. 1999;**96**(6):3104-3107. DOI: 10.1073/pnas.96.6.3104

[24] Tu Y, Chen N, Li C, Liu H, Zhu R, Chen S, et al. Advances in injectable self-healing biomedical hydrogels. Acta Biomaterialia. 2019;**90**:1-20. DOI: 10.1016/j.actbio.2019.03.057

[25] Liu SQ, Ee PL, Ke CY, Hedrick JL, Yang YY. Biodegradable poly(ethylene glycol)-peptide hydrogels with well-defined structure and properties for cell delivery. Biomaterials. 2009;**30**(8):1453-1461. DOI: 10.1016/j.biomaterials. 2008. 11. 023

[26] Stubbe B, Mignon A, Declercq H, Van Vlierberghe S, Dubruel P. Development of gelatin-alginate hydrogels for burn wound treatment. Macromolecular Bioscience. 2019;**19**(8):e1900123. DOI: 10.1002/mabi.201900123

[27] Rowley JA, Madlambayan G, Mooney DJ. Alginate hydrogels as

synthetic extracellular matrix materials. Biomaterials. 1999;**20**(1):45-53. DOI: 10.1016/s0142-9612(98)00107-0

[28] Wiegand C, Heinze T, Hipler UC. Comparative in vitro study on cytotoxicity, antimicrobial activity, and binding capacity for pathophysiological factors in chronic wounds of alginate and silver-containing alginate. Wound Repair and Regeneration. 2009;**17**(4):511-521. DOI: 10.1111/j.1524-475X.2009.00503.x

[29] Zheng WJ, Gao J, Wei Z, Zhou JX, et al. Facile fabrication of self healing carboxymethyl cellulose hydrogels. European Polymer Journal. 2015;**72**(72):514-522. DOI: 10.1016/j.eurpolymj.2015.06.013

[30] Capanema NSV, Mansur AAP, de Jesus AC, Carvalho SM, de Oliveira LC, Mansur HS. Superabsorbent crosslinked carboxymethyl cellulose-PEG hydrogels for potential wound dressing applications. International Journal of Biological Macromolecules. 2018;**106**:1218-1234. DOI: 10.1016/j.ijbiomac.2017.08.124

[31] Xu X, Che L, Xu L, Huang D, Wu J, Du Z, et al. Green preparation of anti-inflammation an injectable 3D porous hydrogel for speeding up deep second-degree scald wound healing. RSC Advances. 2020;**10**(59):36101-36110. DOI: 10.1039/d0ra04990e

[32] Zhang X, Xu L, Huang X, Wei S, Zhai M. Structural study and preliminary biological evaluation on the collagen hydrogel crosslinked by γ-irradiation. Journal of Biomedical Materials Research. Part A. 2012;**100**(11):2960-2969. DOI: 10.1002/jbm.a.34243 Epub 2012 Jun 14

[33] Zhang H, Sun X, Wang J, Zhang Y, Wang L. Multifunctional injectable hydrogel dressings for effectively accelerating wound healing: Enhancing biomineralization strategy. Advanced Functional Materials. 2021:**31**(23):2100093. DOI: 10.1002/adfm.202100093

[34] Stone Ii R, Natesan S, Kowalczewski CJ, Mangum LH, Clay NE, Clohessy RM, et al. Advancements in regenerative strategies through the continuum of burn care. Frontiers in Pharmacology. 2018;**9**:672. DOI: 10.3389/fphar.2018.00672

[35] Homaeigohar S, Boccaccini AR. Antibacterial biohybrid nanofibers for wound dressings. Acta Biomaterialia. 2020;**107**:25-49. DOI: 10.1016/j.actbio.2020.02.022

[36] Chen H, Cheng R, Zhao X, Zhang Y, Tam A, Yan Y, et al. An injectable selfhealing coordinative hydrogel with antibacterial and angiogenic properties for diabetic skin wound repair. NPG Asia Materials. 2019;**11**(1):3. DOI: 10.1038/s41427-018-0103-9

[37] Liu X, Hou M, Luo X, Zheng M, Wang X, Zhang H, et al. Thermoresponsive hemostatic hydrogel with a biomimetic nanostructure constructed from aggregated collagen nanofibers. Biomacromolecules. 2021;**22**(2):319-329. DOI: 10.1021/acs.biomac.0c01167

[38] Ting YH, Chen HJ, Cheng WJ, Horng JC. Zinc(II)-histidine induced collagen peptide assemblies: Morphology modulation and hydrolytic catalysis evaluation. Biomacromolecules. 2018;**19**(7):2629-2637. DOI: 10.1021/acs.biomac.8b00247

[39] Zhu S, Yuan Q, Yin T, You J, Gu Z, Xiong S, et al. Self-assembly of collagen-based biomaterials: Preparation, characterizations and biomedical applications. Journal of Materials Chemistry B. 2018;**6**(18):2650-2676. DOI: 10.1039/c7tb02999c

[40] Yao Y, Zhang A, Yuan C, Chen X, Liu Y. Recent trends on burn wound care: Hydrogel dressings and scaffolds. Biomaterials Science. 2021;**9**(13):4523-4540. DOI: 10.1039/d1bm00411e

[41] Boonkaew B, Barber PM, Rengpipat S, Supaphol P, Kempf M, He J, et al. Development and characterization of a novel, antimicrobial, sterile hydrogel dressing for burn wounds: Single-step production with gamma irradiation creates silver nanoparticles and radical polymerization. Journal of Pharmaceutical Sciences. 2014;**103**(10):3244-3253. DOI: 10.1002/jps.24095

[42] Kim MH, Park H, Nam HC, Park SR, Jung JY, Park WH. Injectable methylcellulose hydrogel containing silver oxide nanoparticles for burn wound healing. Carbohydrate Polymers. 2018;**181**:579-586. DOI: 10.1016/j.carbpol.2017.11.109

[43] Hashmi MU, Khan F, Khalid N, et al. Hydrogels incorporated with silver nanocolloids prepared from antioxidant rich Aerva javanica as disruptive agents against burn wound infections. Colloids & Surfaces A Physicochemical & Engineering Aspects. 2017;**529**(20):475- 486. DOI:10.1016/j.colsurfa.2017.06.036

[44] Lohmann N, Schirmer L, Atallah P, Wandel E, Ferrer RA, Werner C, et al. Glycosaminoglycan-based hydrogels capture inflammatory chemokines and rescue defective wound healing in mice. Science Translational Medicine. 2017;**9**(386):eaai9044. DOI: 10.1126/scitranslmed.aai9044

[45] Schulz A, Fuchs PC, Rothermundt I, Hoffmann A, Rosenberg L, Shoham Y, et al. Enzymatic debridement of deeply burned faces: Healing and early scarring based on tissue preservation compared to traditional surgical debridement. Burns. 2017;**43**(6):1233-1243. DOI: 10.1016/j.burns.2017.02.016

[46] Behrens AM, Sikorski MJ, Li T, Wu ZJ, Griffith BP, Kofinas P. Blood-aggregating hydrogel particles for use as a hemostatic agent. Acta Biomaterialia. 2014;**10**(2):701-708. DOI: 10.1016/j.actbio.2013.10.029

[47] Hong Y, Zhou F, Hua Y, Zhang X, Ni C, Pan D, et al. A strongly adhesive hemostatic hydrogel for the repair of arterial and heart bleeds. Nature Communications. 2019;**10**(1):2060. DOI: 10.1038/s41467-019-10004-7

[48] Weingarten MS, Neidrauer M, Mateo A, Mao X, McDaniel JE, Jenkins L, et al. Prediction of wound healing in human diabetic foot ulcers by diffuse near-infrared spectroscopy: A pilot study. Wound Repair and Regeneration. 2010;**18**(2):180-185. DOI: 10.1111/j.1524-475x.2010.00583.x

[49] Cutting KF, White R. Defined and refined: Criteria for identifying wound infection revisited. British Journal of Community Nursing. 2004;**9**(3):S6-S15. DOI: 10.12968/bjcn.2004.9.Sup1.12495

[50] Zhou A. A survey of optical imaging techniques for assessing wound. The International Journal of Intelligent Control and Systems. 2012;**17**:79-85

[51] Neidrauer M, Papazoglou E. Optical non-invasive characterization of chronic. Bioengineering Research of Chronic Wounds. 2009;**1**:381-404

[52] Kaiser M, Yafi A, Cinat M, Choi B, Durkin AJ. Noninvasive assessment of burn wound severity using optical technology: A review of current and future modalities. Burns. 2011;**37**(3):377-386. DOI: 10.1016/j.burns.2010.11.012

[53] Hsu CK, Tzeng SY, Yang CC, Lee JY, Huang LL, Chen WR, et al. Non-invasive evaluation of therapeutic response in keloid scar using diffuse reflectance spectroscopy. Biomedical Optics Express. 2015;**6**(2):390-404. DOI: 10.1364/BOE.6.000390

[54] Cappon DJ, Farrell TJ, Fang Q, Hayward JE. Fiber-optic probe design and optical property recovery algorithm for optical biopsy of brain tissue. Journal of Biomedical Optics. 2013;**18**(10):107004. DOI: 10.1117/1.JBO.18.10.107004

[55] Cerussi A, Shah N, Hsiang D, Durkin A, Butler J, Tromberg BJ. In vivo absorption, scattering, and physiologic properties of 58 malignant breast tumors determined by broadband diffuse optical spectroscopy. Journal of Biomedical Optics. 2006;**11**(4):044005. DOI: 10.1117/1.2337546

[56] Onozato ML, Andrews PM, Li Q, Jiang J, Cable A, Chen Y. Optical coherence tomography of human kidney. The Journal of Urology. 2010;**183**(5):2009-2004. DOI: 10.1016/j.juro.2009.12.091

[57] Wierwille J, Andrews PM, Onozato ML, Jiang J, Cable A, Chen Y. In vivo, label-free, three-dimensional quantitative imaging of kidney microcirculation using Doppler optical coherence tomography. Laboratory Investigation. 2011;**91**(11):1596-1604. DOI: 10.1038/labinvest.2011.112

[58] Zhao Q, Dai C, Fan S, Lv J, Nie L. Synergistic efficacy of salicylic acid with a penetration enhancer on human skin monitored by OCT and diffuse reflectance spectroscopy. Scientific Reports. 2016;**6**:34954. DOI: 10.1038/srep34954

[59] Marin A, Verdel N, Milanič M, Majaron B. Noninvasive monitoring of dynamical processes in bruised human skin using diffuse reflectance spectroscopy and pulsed Photothermal radiometry. Sensors (Basel). 2021;**21**(1):302. DOI: 10.3390/s21010302

[60] Chen B, Zhang Y, Gao S, Li D. Extraction of the structural properties of skin tissue via diffuse reflectance spectroscopy: An inverse methodology. Sensors (Basel). 2021;**21**(11):3745. DOI: 10.3390/s21113745

[61] Fujimoto J, Swanson E. The development, commercialization, and impact of optical coherence tomography. Investigative Ophthalmology & Visual Science. 2016;**57**(9):OCT1-OCT13. DOI: 10.1167/iovs.16-19963

[62] Wang RK, Jacques SL, Ma Z, Hurst S, Hanson SR, Gruber A. Three dimensional optical angiography. Optics Express. 2007;**15**(7):4083-4097. DOI: 10.1364/oe.15.004083

[63] An L, Qin J, Wang RK. Ultrahigh sensitive optical microangiography for in vivo imaging of microcirculations within human skin tissue beds. Optics Express. 2010;**18**(8):8220-8228. DOI: 10.1364/OE.18.008220

[64] Wang H, Shi L, Qin J, Yousefi S, Li Y, Wang RK. Multimodal optical imaging can reveal changes in microcirculation and tissue oxygenation during skin wound healing. Lasers in Surgery and Medicine. 2014;**46**(6):470-478. DOI: 10.1002/lsm.22254

[65] Park KS, Choi WJ, Song S, Xu J, Wang RK. Multifunctional in vivo imaging for monitoring wound healing using swept-source polarization-sensitive optical coherence tomography. Lasers in Surgery and Medicine. 2018;**50**(3):213-221. DOI: 10.1002/lsm.22767

[66] Oh JT, Lee SW, Kim YS, Suhr KB, Kim BM.Quantification of the wound

healing using polarization-sensitive optical coherence tomography. Journal of Biomedical Optics. 2006;**11**(4):041124. DOI: 10.1117/1.2338826

[67] Adams DC, Szabari MV, Lagares D, McCrossan AF, Hariri LP, Tager AM, et al. Assessing the progression of systemic sclerosis by monitoring the tissue optic axis using PS-OCT. Scientific Reports. 2020;**10**(1):2561. DOI: 10.1038/s41598-020-59330-7

[68] Tack C. Artificial intelligence and machine learning | applications in musculoskeletal physiotherapy. Musculoskeletal Science & Practice. 2019;**39**:164-169. DOI: 10.1016/j.msksp.2018.11.012

[69] Hamet P, Tremblay J. Artificial intelligence in medicine. Metabolism. 2017;**69S**:S36-S40. DOI: 10.1016/j.metabol.2017.01.011

[70] Singh Pathania Y, Budania A. Artificial intelligence in dermatology: "unsupervised" versus "supervised" machine learning. International Journal of Dermatology. 2021;**60**(1):e28-e29. DOI: 10.1111/ijd.15288

[71] Shafique M, Theocharides T, Bouganis CS, Hanif MA, Rehman S. An overview of next-generation architectures for machine learning: Roadmap, opportunities and challenges in the IoT Era. In: 2018 Design, Automation & Test in Europe Conference & Exhibition (DATE). 2018;**1558**(1101):827-832. DOI: 10.23919/DATE.2018.8342120

[72] Khan FH, Ashraf U, Altaf M, Saadeh W. A patient-specific machine learning based EEG processor for accurate estimation of depth of anesthesia. In: 2018 IEEE Biomedical Circuits and Systems Conference (BioCAS). IEEE; 2018

[73] He K, Zhang X, Ren S, Sun J. Delving deep into rectifiers: Surpassing human-level performance on ImageNet classification. Computer Vision and Pattern Recognition. In: Proceedings of the IEEE International Conference on Computer Vision. Santiago, Chile; 2015. pp. 7-13

[74] LeCun Y, Bengio Y, Hinton G. Deep learning. Nature. 2015;**521**(7553):436-444. DOI: 10.1038/nature14539

[75] Marsland S. Machine Learning: An Algorithmic Perspective. 1st. ed. Chapman and Hall/CRC: Massey University Manawatu; 2009. DOI: 10.1016/S0967-2109(97)89838-9

[76] Ray A, Gupta A, Amutha AL. Skin lesion classification with deep convolutional neural network: Process development and validation. JMIR Dermatology. 2020;**3**(1):e18438. DOI: 10.2196/18438

[77] Carvalho TMD, Noels E, Wakkee M, Udrea A, Nijsten T. Development of smartphone apps for skin cancer risk assessment: Progress and promise. JMIR Dermatology. 2019;**2**(1):e13376. DOI: 10.2196/13376

[78] Loescher LJ, Janda M, Soyer HP, Shea K, Curiel-Lewandrowski C. Advances in skin cancer early detection and diagnosis. Seminars in Oncology Nursing. 2013;**29**(3):170-181. DOI: 10.1016/j.soncn.2013.06.003

[79] Lieber CA, Majumder SK, Ellis DL, Billheimer DD, Mahadevan-Jansen A. In vivo nonmelanoma skin cancer diagnosis using Raman microspectroscopy. Lasers in Surgery and Medicine. 2008;**40**(7):461-467. DOI: 10.1002/lsm.20653

[80] Esteva A, Kuprel B, Novoa RA, Ko J, Swetter SM, Blau HM, et al.

Dermatologist-level classification of skin cancer with deep neural networks. Nature. 2017;**542**(7639):115-118. DOI: 10.1038/nature21056

[81] Hormel TT, Hwang TS, Bailey ST, Wilson DJ, Huang D, Jia Y. Artificial intelligence in OCT angiography. Progress in Retinal and Eye Research. 2021;**85**:100965. DOI: 10.1016/j.preteyeres.2021.100965

[82] Dan Y, Wenxin G, Tonglei C, Zhulin W, Bin X. Artificial neural network (ANN) for dispersion compensation of spectral domain – Optical coherence tomography (SD-OCT). Instrumentation Science & Technology. 2022. DOI: 10.1080/10739149.2022.2048008

[83] Haenssle HA, Fink C, Schneiderbauer R, Toberer F, Buhl T, Blum A, et al. Man against machine: Diagnostic performance of a deep learning convolutional neural network for dermoscopic melanoma recognition in comparison to 58 dermatologists. Annals of Oncology. 2018;**29**(8):1836-1842. DOI: 10.1093/annonc/mdy166

[84] Arevalo J, Cruz-Roa A, Arias V, Romero E, González FA. An unsupervised feature learning framework for basal cell carcinoma image analysis. Artificial Intelligence in Medicine. 2015;**64**(2):131-145. DOI: 10.1016/j.artmed.2015.04.004

[85] Kharazmi P, Kalia S, Lui H, Wang ZJ, Lee TK. A feature fusion system for basal cell carcinoma detection through data-driven feature learning and patient profile. Skin Research and Technology. 2018;**24**(2):256-264. DOI: 10.1111/srt.12422

[86] Boone M, Suppa M, Miyamoto M, Marneffe A, Jemec G, Del Marmol V. In vivo assessment of optical properties of basal cell carcinoma and differentiation of BCC subtypes by high-definition optical coherence tomography. Biomedical Optics Express. 2016;**7**(6):2269-2284. DOI: 10.1364/BOE.7.002269

[87] Li A, Cheng J, Yow AP, Srivastava R, Wong DW, Hong Liang T, et al. Automated basal cell carcinoma detection in high-definition optical coherence tomography. In: 2016 38th Annual International Conference of the IEEE Engineering in Medicine and Biology Society (EMBC). 2016. pp. 2885-2888. DOI: 10.1109/EMBC.2016.7591332

[88] Yang Y, Sun J, Li HB. ADMMCS net: A deep learning approach for image compressive sensing. IEEE Transactions on Pattern Analysis and Machine Intelligence. 2020;**42**(3):521-538

[89] Adler J, Öktem O. Learned primal-dual reconstruction. IEEE Transactions on Medical Imaging. 2018;**37**(6):1322-1332

[90] Chen H, Zhang Y, Kalra MK, et al. Low-dose CT with a residual encoderdecoder convolutional neural network. IEEE Transactions on Medical Imaging. 2017;**36**(12):2524-2535

[91] Huang S, Yang J, Fong S, Zhao Q. Artificial intelligence in cancer diagnosis and prognosis: Opportunities and challenges. Cancer Letters. 2020;**471**:61-71. DOI: 10.1016/j.canlet.2019.12.007

[92] Cao C, Liu F, Tan H, Song D, Shu W, Li W, et al. Deep learning and its applications in biomedicine. Genomics, Proteomics & Bioinformatics. 2018;**16**(1):17-32. DOI: 10.1016/j.gpb.2017.07.003

[93] Wang LH, Qin YB. State of the art and future perspectives of the applications of deep learning in the

medical image analysis. Big Data Research. 2020;**6**(6):83-104

[94] Kermany DS, Goldbaum M, Cai W, Valentim CCS, Liang H, Baxter SL, et al. Identifying medical diagnoses and treatable diseases by image-based deep learning. Cell. 2018;**172**(5):1122-1131.e9. DOI: 10.1016/j.cell.2018.02.010

[95] Abdolmanafi A, Cheriet F, Duong L, Ibrahim R, Dahdah N. An automatic diagnostic system of coronary artery lesions in Kawasaki disease using intravascular optical coherence tomography imaging. Journal of Biophotonics. 2020;**13**(1):e201900112. DOI: 10.1002/jbio.201900112

[96] Li J, Yu F, Chen G, Liu J, Li XL, Cheng B, et al. Moist-retaining, self-recoverable, bioadhesive, and transparent in situ forming hydrogels to accelerate wound healing. ACS Applied Materials & Interfaces. 2020;**12**(2):2023-2038. DOI: 10.1021/acsami.9b17180

[97] Korting HC, Schöllmann C, White RJ. Management of minor acute cutaneous wounds: Importance of wound healing in a moist environment. Journal of the European Academy of Dermatology and Venereology. 2011;**25**(2):130-137. DOI: 10.1111/j.1468-3083.2010.03775.x

[98] Feng P, Qiu H, Luo Y, Hu J, Cao Y, Pang Q, et al. Development of Poloxamer hydrogels containing antibacterial guanidine-based polymers for healing of full-thickness skin wound. ACS Biomaterials Science & Engineering. 2021;**7**(9):4557-4568. DOI: 10.1021/acsbiomaterials.1c00600

[99] Shanmugapriya K, Kim H, Kang HW. EGFR-conjugated hydrogel accelerates wound healing on ulcer-induced burn wounds by targeting collagen and inflammatory cells using photoimmunomodulatory inhibition. Materials Science & Engineering. C, Materials for Biological Applications. 2021;**118**:111541. DOI: 10.1016/j.msec.2020.111541

[100] Chen K, Sivaraj D, Davitt MF, Leeolou MC, Henn D, Steele SR, et al. Pullulan-collagen hydrogel wound dressing promotes dermal remodelling and wound healing compared to commercially available collagen dressings. Wound Repair and Regeneration. 2022;**30**(3):397-408. DOI: 10.1111/wrr.13012

[101] Yang L, Lan Y, Guo H, Cheng L, Fan J, Cai X, et al. Ophthalmic drug-loaded N, O-carboxymethyl chitosan hydrogels: Synthesis, in vitro and in vivo evaluation. Acta Pharmacologica Sinica. 2010;**31**(12):1625-1634. DOI: 10.1038/aps.2010.125

[102] Lazarus GS, Cooper DM, Knighton DR, Margolis DJ, Pecoraro RE, Rodeheaver G, et al. Definitions and guidelines for assessment of wounds and evaluation of healing. Archives of Dermatology. 1994;**130**(4):489-493

[103] Zarrintaj P, Khodadadi Yazdi M, Youssefi Azarfam M, Zare M, Ramsey JD, Seidi F, et al. Injectable cell-laden hydrogels for tissue engineering: Recent advances and future opportunities. Tissue Engineering. Part A. 2021;**27**(11-12):821-843. DOI: 10.1089/ten.TEA.2020.0341

[104] Zhao H, Liu C, Gu Z, Dong L, Li F, Yao C, et al. Persistent luminescent nanoparticles containing hydrogels for targeted, sustained, and autofluorescence-free tumor metastasis imaging. Nano Letters. 2020;**20**(1):252-260. DOI: 10.1021/acs.nanolett.9b03755

[105] Chen X, Zhang J, Wu K, Wu X, Ding J. Visualizing the In Vivo Evolution

of an Injectable and Thermosensitive Hydrogel Using Tri-Modal Bioimaging. Small Methods. 2020;**4**(9):2000310. DOI: 10.1002/smtd.202000310

[106] Schwalbe N, Wahl B. Artificial intelligence and the future of global health. Lancet. 2020;**395**(10236):1579-1586. DOI: 10.1016/S0140-6736(20)30226-9

[107] Feng H, Gu ZY, Li Q, Liu QH, Yang XY, Zhang JJ. Identification of significant genes with poor prognosis in ovarian cancer via bioinformatical analysis. Journal of Ovarian Research. 2019;**12**(1):35. DOI: 10.1186/s13048-019-0508-2

[108] Yow AP, Srivastava R, Cheng J, Li A, Liu J, Schmetterer L, et al. Techniques and applications in skin OCT analysis. Advances in Experimental Medicine and Biology. 2020;**1213**:149-163. DOI: 10.1007/978-3-030-33128-3_10